

#### **Mechanical and tribological properties of CNTs coated aramid FREC**

This chapter presents the physical, mechanical, thermal, and tribological properties of fabricated aramid fiber-reinforced polymer composites. These properties were evaluated through density measurements, tensile testing, hardness testing, thermal conductivity analysis, and tribological assessments. SEM analysis was further conducted to examine the worn surfaces of composite samples, providing insights into their wear mechanisms and surface morphology. These comprehensive characterizations contribute to understanding the behavior of the composite materials under various conditions, highlighting their potential for various applications.

#### **4.1. FTIR analysis**

##### **4.1.1. Infrared Spectroscopy of CNT**

FTIR analysis was done on chemically treated (functionalized CNT) and untreated CNT and their corresponding spectra, as shown in Figure 4.1. Fourier Transform Infrared Spectroscopy is the most common technique for identifying functional groups on chemically functionalized CNT. On samples of functionalized CNTs, a thorough FTIR investigation is carried out. FTIR analysis is performed in between 500 to 4000  $\text{cm}^{-1}$  wave number. For untreated CNT Figure 4.1(a), the IR spectrum shows the peak at 3436  $\text{cm}^{-1}$  is attributed to the O-H stretching [187]. The peak at 1630  $\text{cm}^{-1}$  is attributed to C=C aromatic stretching [188, 189]. The peak at 2919  $\text{cm}^{-1}$  is attributed to the CH<sub>2</sub> stretching, and the peak at 1076  $\text{cm}^{-1}$  is attributed to the C-O groups [190]. The peak at 674  $\text{cm}^{-1}$  also indicated the S=O stretching mode of the -SO<sub>3</sub>H group [191, 192]. Additionally, Figure 4.1(b)

demonstrates the same infrared peak after the oxidation treatments despite some intensity variations and, occasionally, the appearance of new peaks. In Figure 4.1(b), 10 M mixture of sulphuric and nitric acids was used for the chemical treatment of CNT, which showed the same peak along with this, a new intensity peak at  $1725\text{ cm}^{-1}$ , which can be associated with the stretching vibrations of carbonyl groups (C=O) found in carboxylic acids (RCOOH), which is absent in untreated CNT [187]. The peak at  $3436\text{ cm}^{-1}$  (O-H stretching) of functionalized CNT is increased compared to untreated CNT.

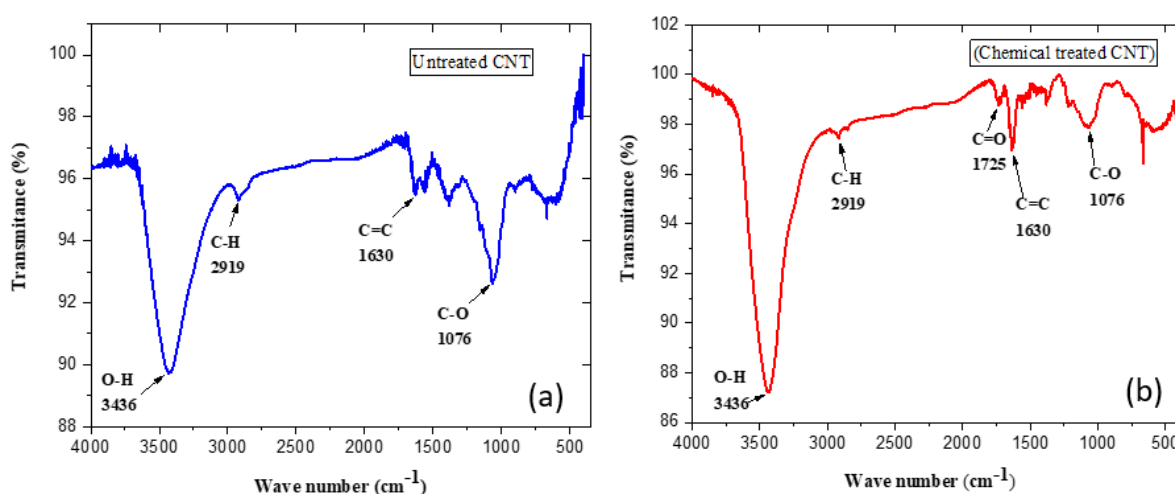


**Figure 4.1** FTIR spectra of (a) Untreated CNT, (b) Chemically treated CNT

#### 4.1.2. Infrared Spectroscopy of aramid Fiber

Figure 4.2 shows the FTIR analysis of untreated aramid fiber and chemically treated (functionalized) aramid fiber, which is performed in between  $500$  to  $4000\text{ cm}^{-1}$  wave number. In Figure 4.2, the peak at  $1109\text{ cm}^{-1}$  and  $1306\text{ cm}^{-1}$  is associated with the stretching vibration of the C-N bonds [193]. Stretching vibration of the C=O and N-H groups corresponds to the peaks at  $1639\text{ cm}^{-1}$  and  $1514\text{ cm}^{-1}$ , respectively [193, 194]. The combined motion of C-N and N-H bending is linked to the absorption peak at  $1537\text{ cm}^{-1}$  [195]. Stretching vibrations of the amide group's N-H is responsible for the absorption band at  $3316\text{ cm}^{-1}$  [194]. When untreated aramid fiber was submerged in a 3 M solution of

sulphuric and nitric acids, the sizing agent on the fiber was removed, as indicated by the lower intensity of the stretching vibrations of the methyl and methylene groups at  $2922\text{ cm}^{-1}$  and  $2854\text{ cm}^{-1}$  in the treated fiber compared to the untreated fiber [196]. The stretching vibrations of the C-H bonds inside the aromatic ring that forms the backbone structure of the aramid fiber are also associated with the absorption band at  $820\text{ cm}^{-1}$ . When the fiber is subjected to chemical treatments, this band's intensity does not show any noticeable alterations [195]. The treated aramid fiber attributed to the new absorption peak at  $3445\text{ cm}^{-1}$ , as shown in Figure 4.2(b), which was assigned to the hydroxyl group O-H which is not observed in untreated aramid fiber. At the same time, the peak at  $3316\text{ cm}^{-1}$  (N-H),  $1306\text{ cm}^{-1}$  (C-N), and  $824\text{ cm}^{-1}$  (C-H) had a higher intensity peak in treated aramid fiber than that in untreated aramid fiber [197].

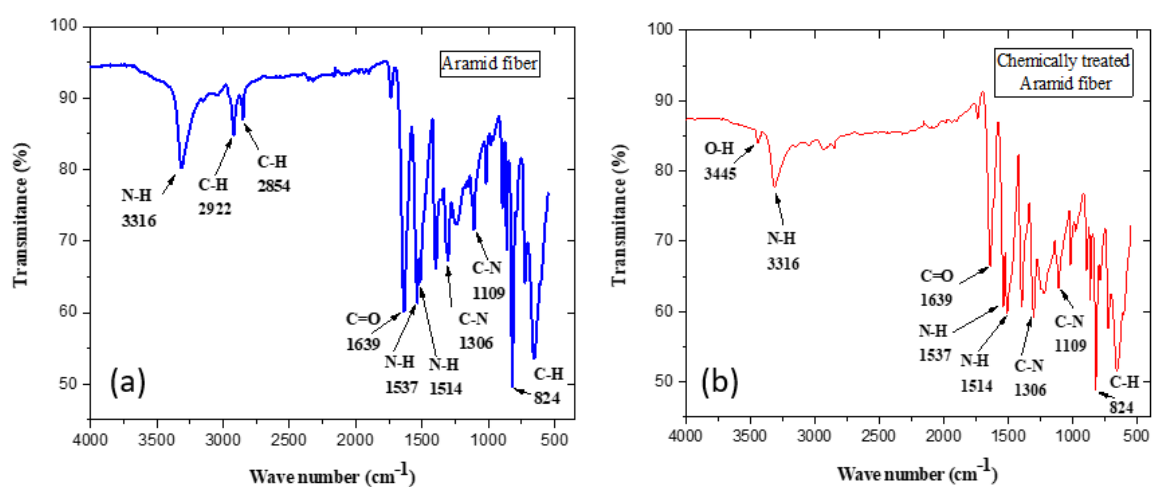


**Figure 4.2** FTIR spectra of (a) Untreated aramid fiber, (b) Chemically treated aramid fiber

## 4.2. TGA analysis of aramid fiber and CNT-coated aramid fiber

The TGA curve of aramid fiber and CNT-coated aramid fiber is shown in Figure 4.3. In a TGA curve, the plateau zone denotes the fiber thermal stability interval, while the steep stage denotes the weight loss period. The thermogravimetric curves from  $24\text{ }^{\circ}\text{C}$  to  $800\text{ }^{\circ}\text{C}$  included three stages, as shown in Figure 4.3. The removal of some waxy

components and moisture contents from the fibers led to the first stage of thermal deterioration, which occur between 24 °C and 540 °C, with a weight loss of around 5–6% in this temperature range for both uncoated aramid fiber and CNT coated aramid fiber [198]. The second degradation (decomposed sharply) stage occurred at a temperature range between 540 °C to 640 °C, mainly caused by partial de-hydroxylation and alkoxide decomposition of the aramid fiber [28, 199]. In this temperature range, uncoated aramid fiber lost roughly 32% of its weight. In contrast, CNT-coated aramid fiber lost approximately 28% of its weight, which is less than uncoated aramid fiber because of the high thermal stability of CNT, which can potentially enhance the overall thermal stability of the fiber. The last stage of degradation occurs between 640 °C to 800 °C and corresponds to the loss of the amide group in aramid fiber [200]. Aramid fiber lost roughly 28% of its weight in this temperature range, and CNT-coated aramid fiber lost approximately 13%. The weight loss is reduced in CNT-coated aramid fiber because the CNT coating acts as a protective barrier, potentially delaying or hindering the degradation of the aramid fiber by providing a thermal barrier. The overall weight loss of uncoated and coated aramid fiber is 66% and 48%, respectively. This suggests that the coating of CNT can increase the thermal stability of aramid fiber on it.

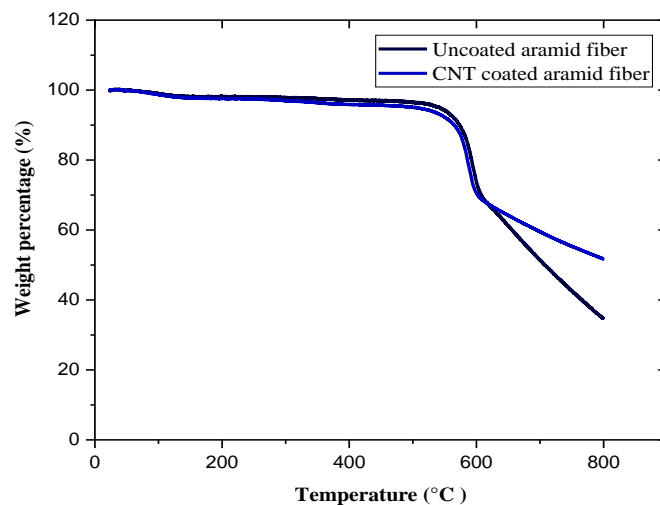


**Figure 4.3** TGA curves of uncoated aramid fiber and CNT-coated aramid fiber

### 4.3 Scanning electron microscopy (SEM)

Using FE-SEM, the structural and morphological investigation of CNTs has been examined. Figure 4.4 depicts the impact on the carbon nanotubes' surface before and after acid treatment. The acid functionalization method has caused minimal alterations in the structure of carbon nanotubes, as observed in the FE-SEM images, in comparison to the original, as-synthesized CNTs. After the functionalization procedure, the smooth surface of the carbon nanotubes, as shown in Figure 4.4(a), may change to look like a groovy surface, as shown in Figure 4.4(b), which may be connected to the chemical functional groups attached on the carbon nanotubes surface [201]. The functionalization of CNT was also confirmed by the attachment of functional group from the FTIR analysis as shown in Figure 4.1. Comparing functionalized CNTs to as-synthesized CNTs, the transparency of carbon nanotubes is also reduced, which may be connected to the addition of functional groups [201, 202]. From the FE-SEM image of functionalized CNT samples, it observed that structure is still preserved, regarding tube shortening by the acidic oxidation process [201, 203]. The surface morphology of chemically treated aramid fiber after the dip coating of functionalized CNT was studied by SEM study, as shown in Figure 4.5. Figure 4.5(a) shows the clean SEM image of chemically treated aramid fiber. The morphology of CAF with surface modification had significantly changed after the deposition of FCNTs on the surface of fiber by dip coating, as illustrated in Figure 4.5(b). FCNTs were randomly orientated and wrapped around the initially clean surface of chemically treated aramid fiber, creating a rougher surface with many protrusions [66]. SEM micrograph of CAF-FCNTs fiber has a uniform distribution of FCNTs on the fiber surface with some agglomerates observed.

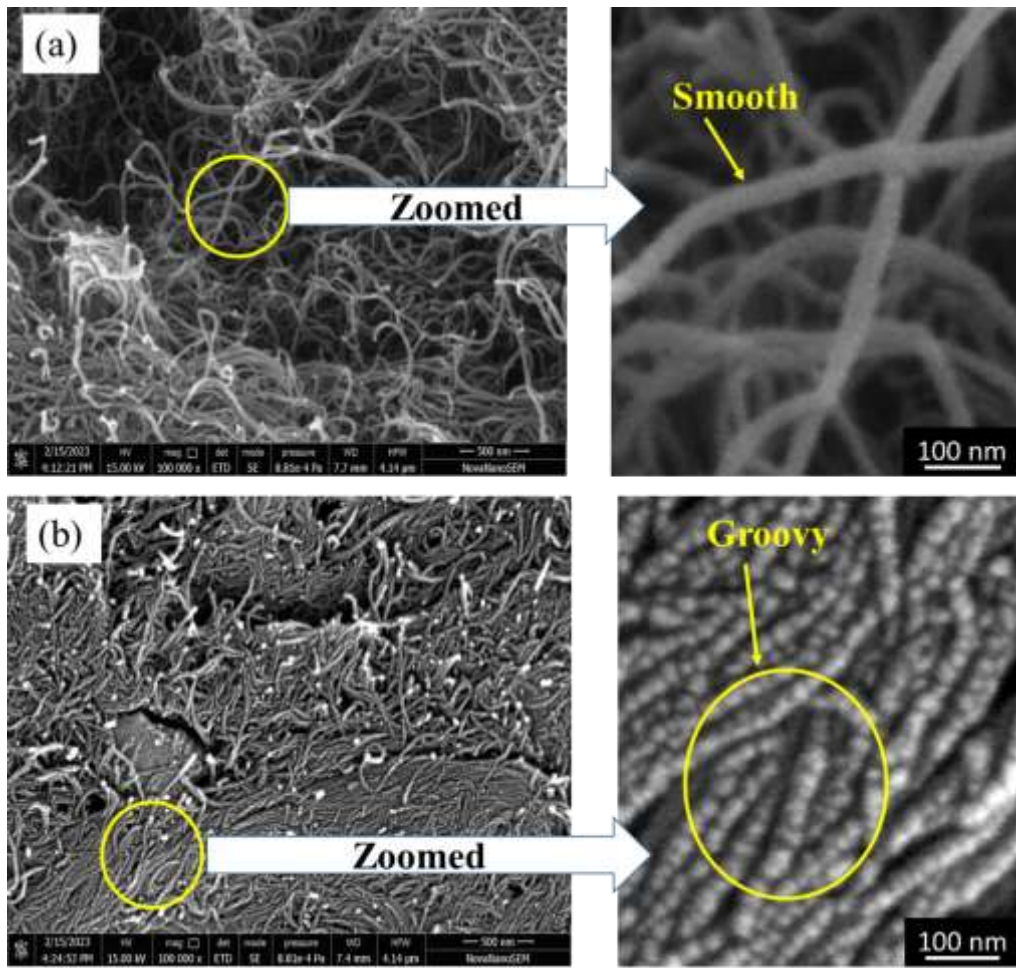


**Figure 4.4** FE-SEM images of (a) CNT, (b) FCNTs

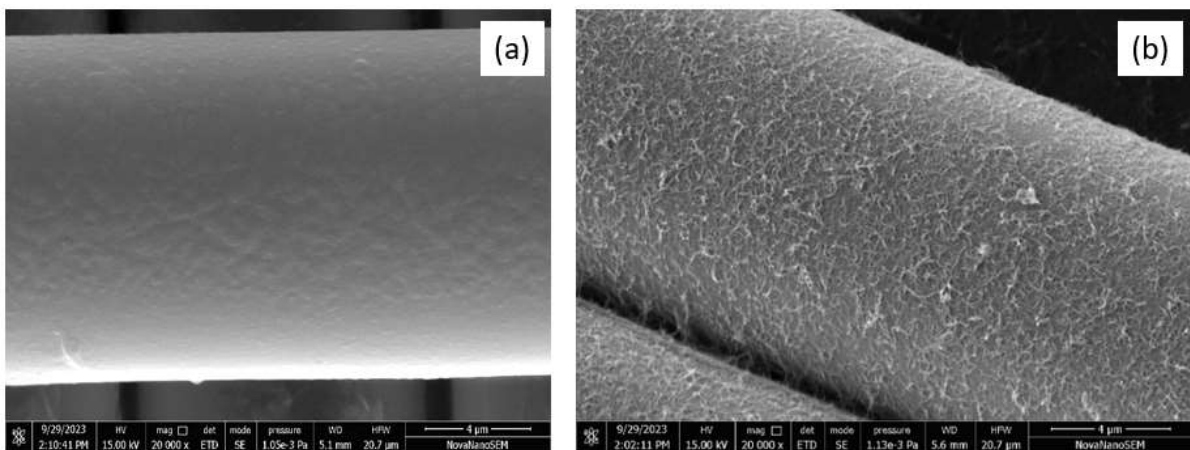


**Figure 4.5** FE-SEM micrograph of (a) CAF, (b) CAF-FCNTs

#### 4.4 Density calculation

The specific gravity and density of the polymer composites (CAF-FCNT/Epoxy and AF/Epoxy) are shown in Table 4.1. The density of CAF-FCNT/Epoxy and AF/Epoxy polymer composites samples are averaged and found to be 1153.0305 kg/m<sup>3</sup> and 1177.9056 kg/m<sup>3</sup>, respectively. In comparison to AF/Epoxy, CAF-FCNT/Epoxy composites have a lower density.

**Table 4.1.** Density calculation CAF-FCNT/Epoxy and AF/Epoxy polymer composites

S.No.	CAF-FCNT/Epoxy (mass in the air) (Gram)	CAF-FCNT/Epoxy (mass immersed in water) (Gram)	Specific Gravity	Density (Kg/m <sup>3</sup> )
1.	1.324	0.180	1.1573	1153.8281
2.	1.358	0.183	1.1557	1152.2329
S.No.	AF/Epoxy (mass in the air) (Gram)	AF/Epoxy (mass immersed in water) (Gram)	Specific Gravity	Density (Kg/m <sup>3</sup> )
1.	1.543	0.241	1.1851	1181.5447
2.	1.610	0.243	1.1778	1174.2666

#### 4.5 Microhardness test

A square shape specimen with a (20mm X 20mm) cross-section is extracted from the center of both the polymer composite sample. Subsequently, the extracted square specimen is subjected to a cleaning process using acetone to eliminate any contaminants or impurities adhering to its surface. Subsequently, this cleaned specimen is employed for

conducting a hardness test. The surface of the specimen was marked with 5 distinct indentations for both the composite samples. Micro-hardness measurements were taken at each spot, so the average of 5 readings was taken for each sample as shown in Figure 4.6. It can be also concluded from Figure 4.7 that the hardness of AF/Epoxy gets increased from  $22 \pm 2$  HV to  $28 \pm 2$  HV in CAF-FCNT/Epoxy sample by the coating of CNTs on AF.

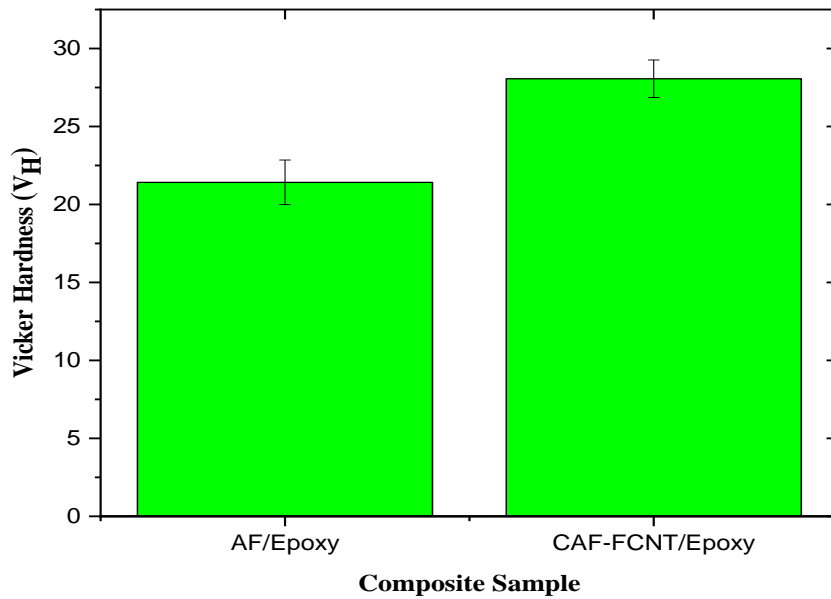


**Figure 4.6** Vickers hardness value for AF/epoxy and CAF-FCNT/Epoxy polymer composites

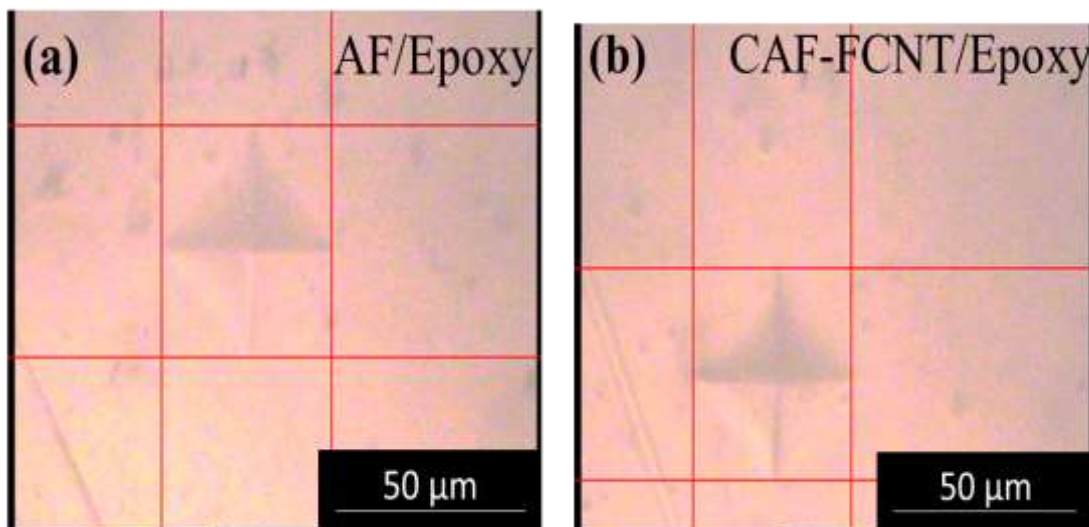


**Figure 4.7** Microhardness indentation images of (a) AF/epoxy, (b) CAF-FCNT/Epoxy.

The mechanical coupling between the fiber and matrix has enhanced due to the bridging action of CNTs, increasing the hardness [204]. Additionally, the CNT coating on aramid fiber significantly improves the bonding between the fiber and epoxy [66]. Providing resistance to the movement of the interface shear bonds reduces the possibility of deformation caused by external forces. As a result, the polymer composite becomes harder.

#### **4.6 Tensile testing**

The tensile test of the AF/Epoxy and CAF-FCNT/Epoxy was carried out to evaluate the reinforcing effects of the bidirectional woven AF and bidirectional woven hybrid CAF-FCNT fiber on the tensile property of the resulting polymer composite laminates. The typical stress-strain curves for the AF/Epoxy and CAF-FCNT/Epoxy materials are shown in Figure 4.8. The composite is noticeably brittle as shown in the measured strain's size. The addition of the CNTs and their presence made the composite even more brittle while simultaneously making it stronger, as seen by the composite's greater failure stress [205]. The tensile strength and tensile modulus values derived from the stress-strain curve are shown in Figure 4.9. Compared to AF/Epoxy, the CAF-FCNT/Epoxy exhibits greater tensile modulus and tensile strength. CNTs improve the load-bearing capacity of a composite by enhancing the adhesion between aramid fibers and epoxy through a process known as bridging [204]. This means that the CNTs act as a mediator between the fibers and epoxy, resulting in a stronger bond and a more resilient composite material. The maximum tensile strength of the CAF-FCNT /Epoxy composite is 310.19 MPa, which is 23.3% greater than that of the AF/Epoxy composite. The tensile strength of polymer composite laminates can be enhanced by different factors, including the robustness of the matrix material, the quality of interfacial adhesion, and the effective dispersion of fibers or particles within the matrix [206]. Because of the smooth surface of AF, which exhibits weak interfacial adhesion between its matrix and fiber strand, So the deposition of FCNT

to the CAF results in better interfacial bonding between fiber and epoxy, which helps to transfer stress more effectively from the epoxy to the fiber [207].

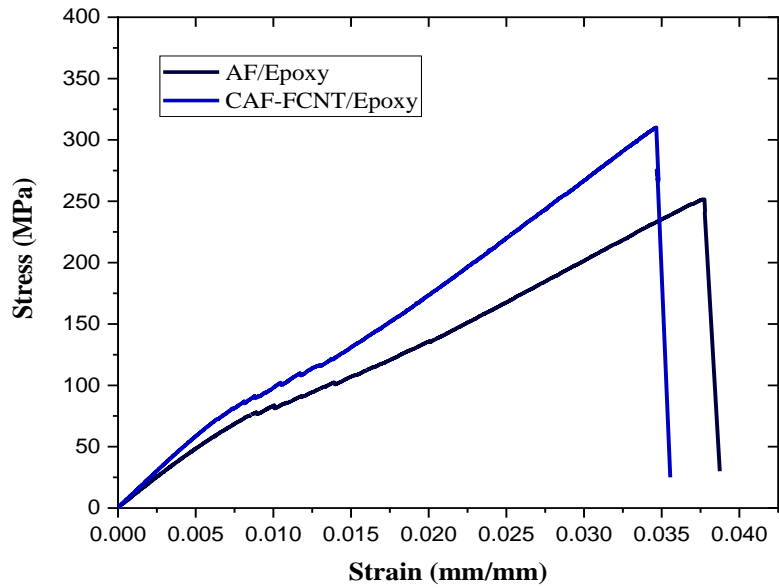


**Figure 4.8.** Stress-strain curves of AF/Epoxy and CAF-FCNT/Epoxy polymer composites

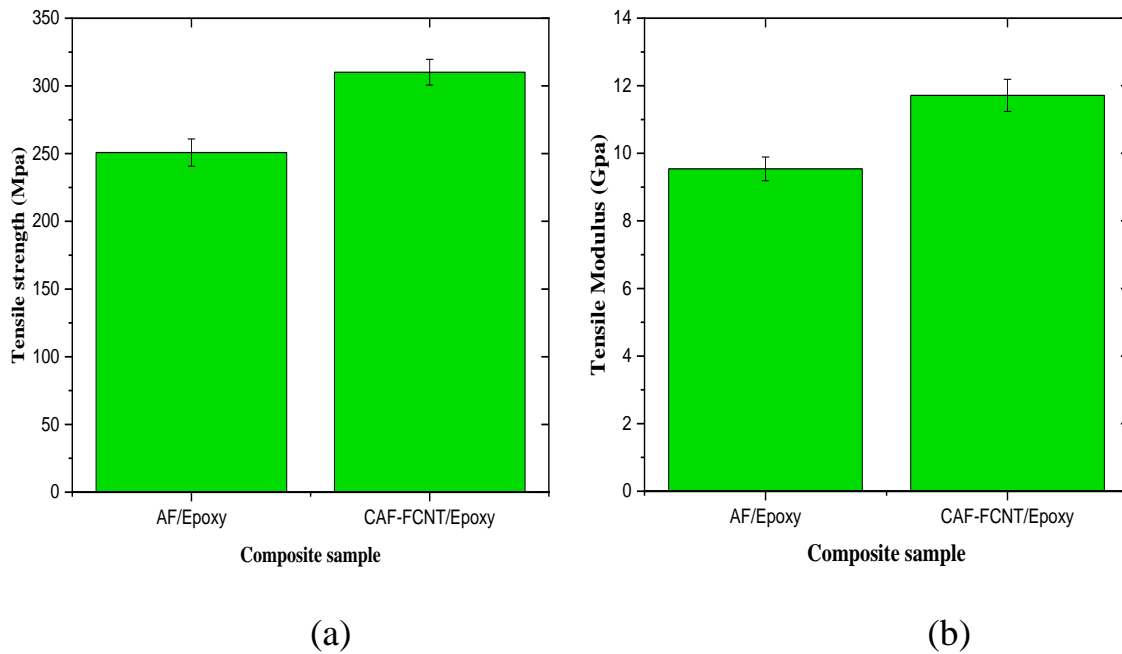


**Figure 4.9** Tensile strength and tensile modulus of AF/Epoxy and CAF-FCNT/Epoxy polymer composites

This results to an improvement in the tensile strength of the composite material. CNT that has been deposited offers a larger surface area at the interface between the fiber

and matrix, leading to enhanced interlocking. This, in turn, improves the adhesion at the interface. The inclusion of carbon nanotubes (CNTs) in woven aramid fiber composites improves the surface roughness of the fiber, allowing it to withstand loads better and enhancing the transmission of stress between the fiber and epoxy matrix. The twisted and kinked structure of CNTs creates mechanical interlocks with the epoxy matrix [208]. Due to the remarkable mechanical properties of CNTs, it was anticipated that incorporating CNTs into the composite (CAF-FCNT/Epoxy) would result in increased tensile strength [209]. The increase in tensile modulus observed in AF/Epoxy and CAF-FCNT/Epoxy materials follow a similar trend as the increase in tensile strength. In particular, the CAF-FCNT/Epoxy material exhibits the highest tensile modulus of 11.70 GPa, corresponding to a relative increase of about 22.9% compared to AF/Epoxy. The FCNTs on the surface of the CAF, which prevent the polymer chain from moving under load, are responsible for the improvement in tensile modulus [210]. Additionally, CNTs were present, which boosted the cross-linking ratio and prevented the epoxy matrix's molecules from moving [211]. The increased surface area of the fiber and the strength of the CNT also improved tensile modulus.

#### **4.7 Thermal conductivity**

Thermal conductivity tests were conducted for both AF/Epoxy and CAF-FCNT/Epoxy composites. Square-shaped samples with a (20mm X 20mm) cross-section were taken from both the fabricated polymer composite specimens, which had uniform and flat surfaces, as shown in Figure 4.10. From the bar chart, as shown in Figure 4.11, it can be noted that the thermal conductivity of CAF-FCNT/epoxy is higher than that of AF/epoxy. This difference may be explained by elements such as the nanofillers' dispersion, alignment, and thermal contact resistance with the matrix. The shape,

alignment, weight percentage, thermal contact resistance and the level of dispersion of the particles inside the composite material have an impact on its thermal conductivity. The presence of well-aligned and dispersed nanofillers, particularly carbon nanotubes (CNTs), creates a well-connected network that facilitates the diffusion of phonons and enhances heat conduction within the CAF-FCNT/epoxy composite. As a result, the thermal conductivity gradually increases in the CAF-FCNT/epoxy composite compared to the AF/epoxy composite.



**Figure 4.10** Thermal conductivity samples of (a) AF/Epoxy, (b) CAF-FCNT/Epoxy

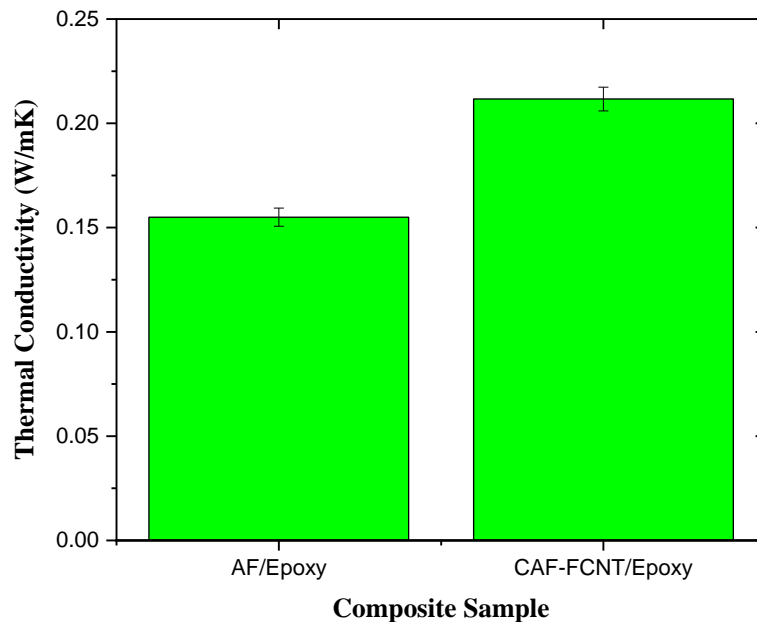


**Figure 4.11** Thermal conductivity of AF/Epoxy and CAF-FCNT/Epoxy

## 4.8 Tribological testing

### 4.8.1 Impact of CNT coating on the tribological properties of aramid fiber reinforced polymer composites

Figure 4.12 shows the changes in the friction coefficient of CAF-FCNT/epoxy and AF/epoxy composites over time. The test was performed at 30°C for 9600 cycles, with a normal load of 40 N, a frequency of reciprocating motion of 8 Hz, and a reciprocating length of 1.5 mm. The results indicate that initially, the friction coefficient increased for both composites due to the plasticization of the matrix, which caused the adhesion of the matrix to the surface of the steel ball and delamination of the composite material's surface [212]. However, after a few cycles, aramid fiber fragments formed, acting as third-body particles, and the friction coefficient was significantly reduced before stabilizing. These fiber particles repeatedly spun between the interacting surfaces, forming a friction layer that decreased the coefficient of friction and stabilized it over time. Furthermore, it was observed that the COF of the CAF-FCNT/epoxy polymer composites was lower as compared to AF/epoxy. The CNTs self-lubricating properties led to the creation of a carbon film on the contacting surfaces, which reduced both the friction and wear rate [213]. From Figure 4.13, it can be noted that the CAF-FCNT/epoxy composite exhibits lower weight loss and specific wear rate than that of the AF/epoxy composite under the same testing condition (40 N, 8Hz, 30°C). This can be attributed to the presence of CNTs, which were coated on the aramid fiber in the CAF-FCNT/epoxy composite. This enhanced the interfacial adhesion, ultimately leading to increased wear resistance. The formula for calculating the specific wear rate is given by Equation 4.1, also called Archard's as given below [214]:

$$\text{Specific wear rate (Ws)} = \frac{V}{WD} \quad \left(\frac{m^3}{Nm}\right) \quad (4.1)$$

Where,  $V$  is the wear volume,  $W$  is the normal load, and  $D$  is the distance travelled.

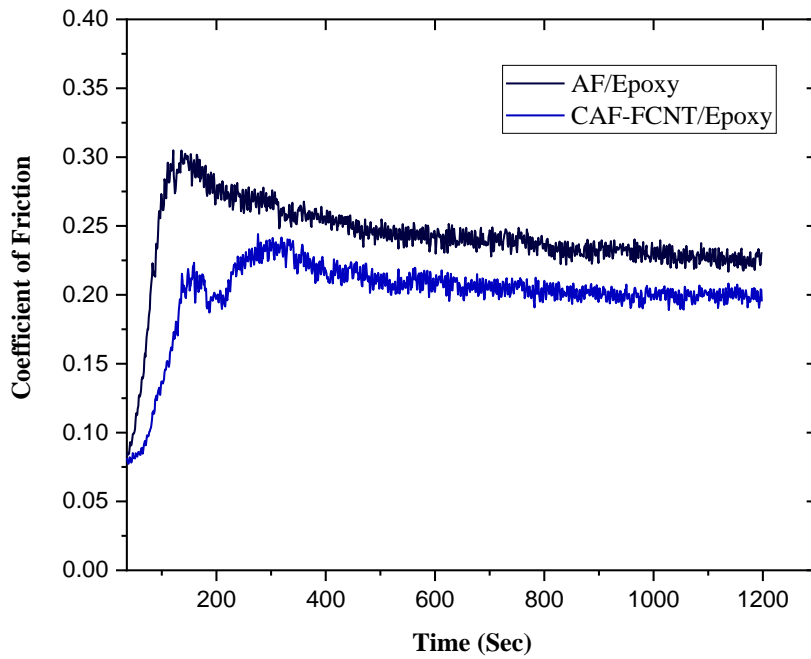


**Figure 4.12** Variation of COF with time for AF/epoxy and CAF-FCNT/epoxy polymer composite at (40 N, 8Hz, 30°C)

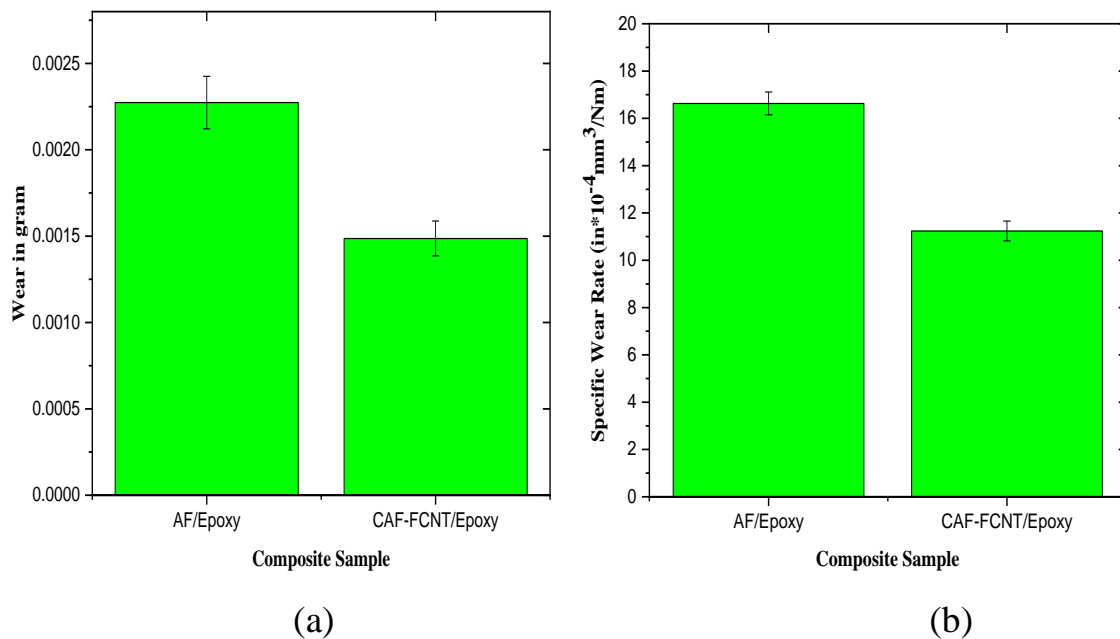


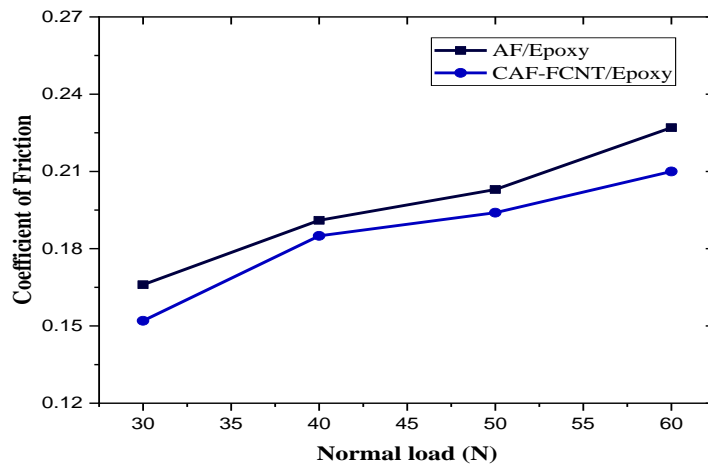
**Figure 4.13** Variation of (a) wear in gram and (b) specific wear rate of AF/epoxy and CAF-FCNT/epoxy at (40 N, 8Hz, 30°C)

During sliding action, the aramid fiber experiences rolling behavior, while the CNTs provide layered shear on the sliding path, creating a thin film. This film reduces sliding wear. A tribological film was generated by incorporating carbon nanotubes (CNTs) into phenolic resin. It was also observed by Wang et al. [215] that the tribological abilities are improved by the rod-like CNT, which has the potential to efficiently toughen the polymer composites and exert a superior lubricating effect on worn surfaces. As a result, adding CNTs to a base material decreases the wear volume loss of the material and the system's COF, which is facilitated by the drop in the coefficients of adhesion and deformation [216].

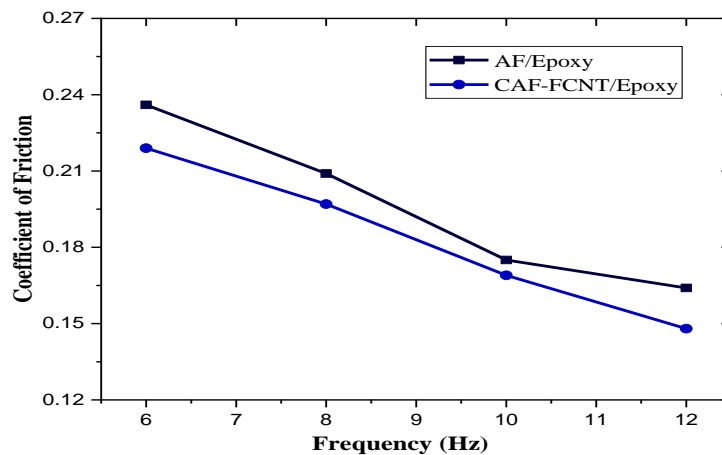
#### **4.8.2. Impact of different parameters (frequency, normal load and temperature) on the friction properties of polymer composites**

Figure 4.14 shows the COF values of AF/epoxy and CAF-FCNT/epoxy under a constant frequency of 8 Hz and a constant temperature of 30° C at different applied normal loads (30, 40, 50, and 60 N). It is observed that when the applied normal load increases, the COF of the polymer composite samples (AF/epoxy and CAF-FCNT/epoxy) increases. It is possible that when there is an increase in contact pressure between the specimen and the steel ball at higher loads, the temperature at the interface may also increase, this causes the friction's adhesion component to rise [217]. Apart from this, the friction coefficient's abrasion component also increased significantly at higher loads due to the significant penetration of asperities, which increased frictional force. This could be a potential explanation for an increase in the coefficient of friction at higher loads. Under a normal load of 30 N, the CAF-FCNT/epoxy composite shows the lowest friction coefficient value of 0.152, while the AF/epoxy composite shows the highest friction coefficient value of 0.227. Figure 4.15 shows the variation of friction coefficient with respect to frequency of AF/epoxy and CAF-FCNT/epoxy polymer composites under a normal uniform load of 40

N and constant temperature of 30° C. From Figure 4.15, it is observed that the COF of the polymer composites sample (AF/epoxy and CAF-FCNT/epoxy) decreases with the increase in sliding frequency. This attributed that the frequency of reciprocating sliding has increased, resulting in greater softening and plastic deformation of the polymer matrix. Adding aramid fibers to the polymer composite significantly reduces its adhesion force and plowing action, leading to superior friction characteristics. Guo et al. [218] also observed that the COF decreases with sliding frequency, which is attributed to the surface softening caused by frictional heating.



**Figure 4.14** Variation of COF with load at a constant temperature and frequency of 30° C and 8 Hz, respectively



**Figure 4.15** Variation of COF with frequency at a constant temperature and load of 30° C and 40N, respectively

The CAF-FCNT/epoxy at 12 Hz recorded the lowest friction coefficient value of 0.148, while the AF/epoxy at 6 Hz recorded the highest friction coefficient value of 0.236. Figure 4.16 shows the variation of friction coefficient with respect to temperature of AF/epoxy and CAF-FCNT/epoxy polymer composites under a load of 40 N and a sliding frequency of 8 Hz. From Figure 4.16, it is observed that the COF of the polymer composites sample (AF/epoxy and CAF-FCNT/epoxy) decreases with the increase in temperature. At high temperatures, the softening and melting of the polymer matrix can result in reduced contact between the specimen and the opposing surface, leading to reduced friction. In addition, at high temperatures, the fibers themselves may begin to soften and reduce the resisting force as the temperature increases, further reducing the coefficient of friction [213]. The minimum friction coefficient value of 0.154 was recorded by CAF-FCNT/epoxy at 60°C, while the maximum friction coefficient value of 0.197 was recorded by AF/epoxy at 30°C.

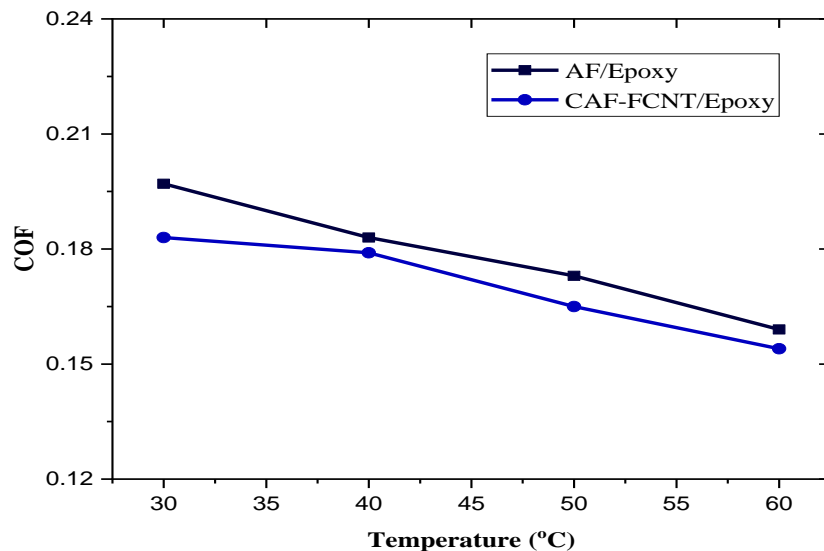
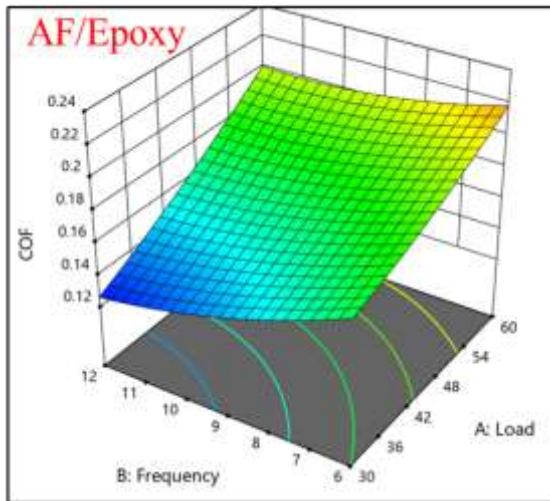


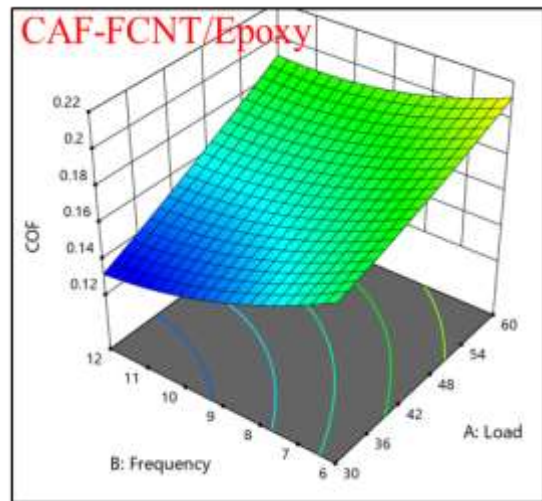
**Figure 4.16.** Variation of COF with the temperature at a constant frequency and load of 8 Hz and 40N, respectively

Figures 4.14, 4.15, 4.16, and 4.17 also showed that the friction coefficient of CAF-FCNT/epoxy polymer composites was lower as compared to AF/epoxy, because of the self-

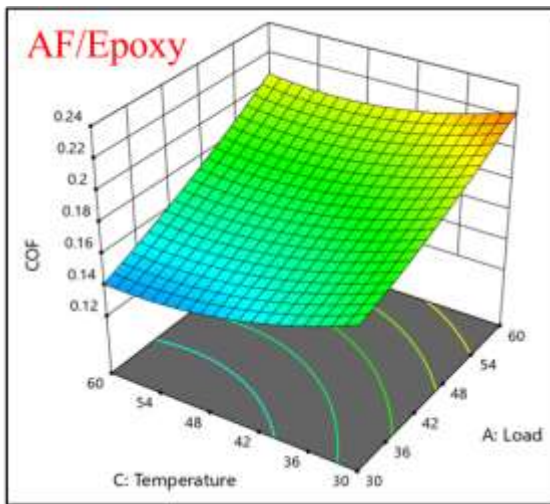
lubricating properties of CNTs, which led to the creation of a carbon film on the contacting surfaces, and the improvement of interfacial adhesion between the CNT coated aramid fiber and matrix which reduced the friction. The coefficient of friction (COF) at three various parameters, such as load, temperature, and frequency, and combining these three parameters in a 3D surface profile, as shown in Figure 4.17, provides a visual representation of the complex interplay between load, temperature, and frequency on the COF. It allows for a better understanding of the tribological behavior of the system and can help identify optimal operating conditions or design improvements to enhance frictional performance. The figures illustrate distinct trends in the coefficient of friction (COF) within various conditions. In Figures 4.17(a) and (b), the COF decreases with increased frequency and reduced load. At higher loads, friction's adhesion component rises, which is countered by a rise in frequency, which softens the contact surface, ultimately reducing the COF. Figures 4.17(c) and (d) reveal a reduction in COF with increasing temperature due to polymer softening, which diminishes material adhesion at elevated loads. However, at a specific temperature, COF rises with increased load, attributed to abrasion caused by the penetration of asperities. Figures 4.17(e) and (f) demonstrate a reduction in COF with increasing frequency and temperature, as increased frequency softens the material and elevated temperature increases flow ability, promoting a lubrication effect. So, the combined effect of increased temperature and frequency reduces COF. The optimal operating conditions for minimizing friction in both AF/Epoxy and CAF-FCNT/Epoxy composites appear to be characterized by lower loads, higher frequencies, and elevated temperatures. Furthermore, the data in Figure 4.17 consistently indicate that the coefficient of friction (COF) is generally lower for CAF-FCNT/Epoxy compared to AF/Epoxy. These findings suggest that CAF-FCNT/Epoxy composites exhibit superior friction-reducing properties across a range of conditions.



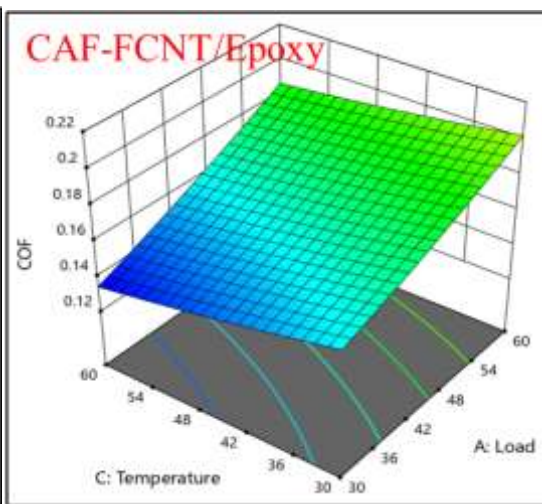
(a)



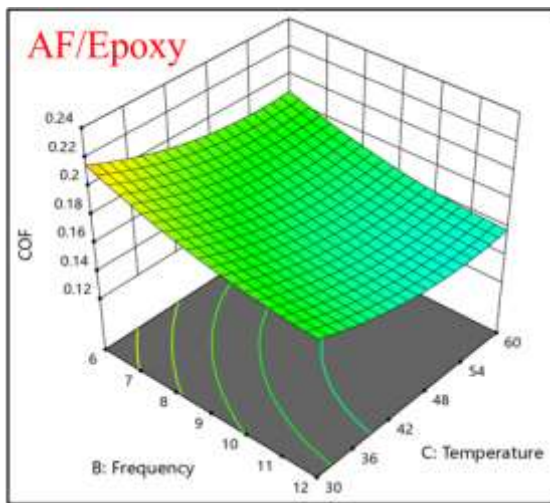
(b)



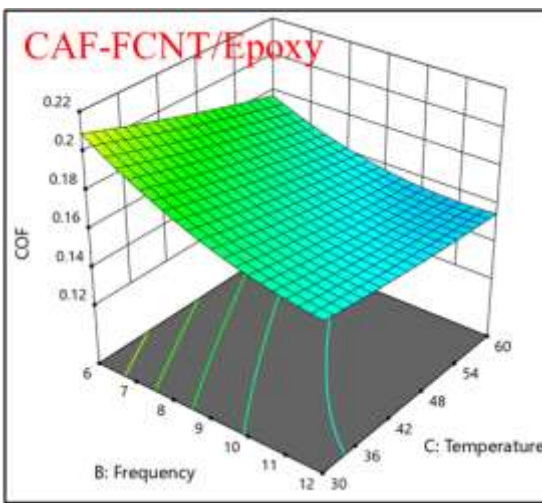
(c)



(d)



(e)



(f)

**Figure 4.17** 3D surface profile of COF at two different parameters simultaneously (a), (c), and (e) is AF/epoxy and (b), (d), and (f) is CAF-FCNT/epoxy composites.

#### 4.9 SEM analysis of worn surface

The worn surfaces of composites made of AF/epoxy and CAF-FCNT/epoxy were examined under various conditions. When the tribological test was performed under the testing condition of 40 N load, 30°C temperature, and 8 Hz frequency. It was observed that the matrix material started to delaminate at an early stage, which was indicated in Figure 4.18(a). This happened as a result of the matrix material plasticizing, which made it stick to the opposing surface since the early cycles' COF was high. As the cycles proceeded, aramid fiber pieces were created, as seen in Figure 4.18(b), which caused the COF to drop. When the fibers were in close touch with the opposing surface and broke off, these pieces were produced. When the resultant fiber pieces rolled between the contacting surfaces, they behaved as particles and contributed as a third body to the wear process.

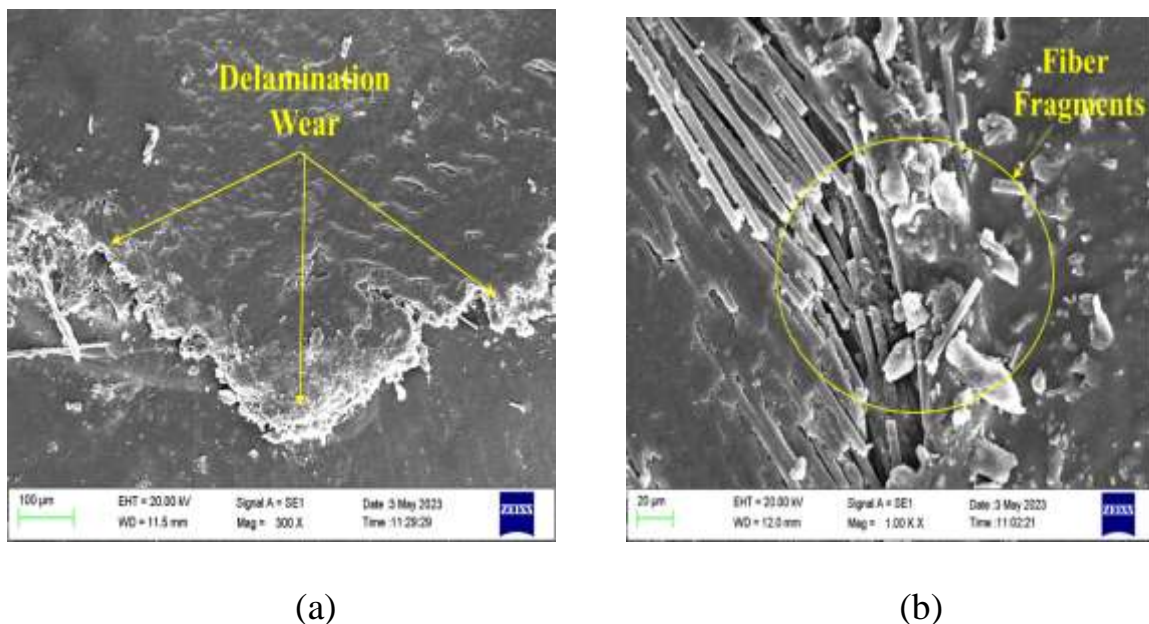


**Figure 4.18** SEM images of the wear surface of the CAF-FCNT/Epoxy sample were tested at 40 N load, 30°C temperature, and 8 Hz frequency (a) Delamination wear, (b) Fiber fragments

Figure 4.19 shows the scanning electron microscope of the worn surface of AF/epoxy and CAF-FCNT/epoxy. After performing the tribological test for both the specimens under the same testing conditions of load, sliding frequency, and temperature (50 N, 8 Hz, 30°C), it was found that AF/epoxy composites as shown in Figure 4.19(a) exhibited more significant matrix layer removal as well as fiber breakage in comparison to CAF-FCNT/epoxy composites as shown in Figure 4.19(b).

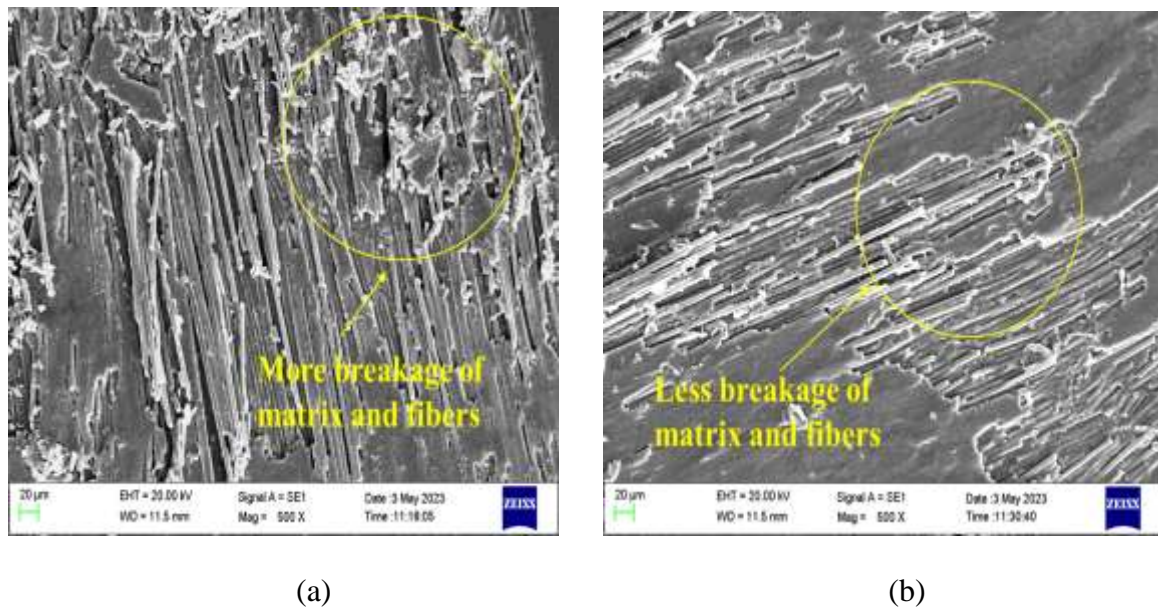


**Figure 4.19.** SEM photo of the worn surface under the same condition of (50 N, 8 Hz, 30°C) (a) AF/epoxy and (b) CAF-FCNT/epoxy composite

This difference in CAF-FCNT/epoxy composites is due to the fact that CNTs are coated to the aramid fibers, enhancing the mechanical interlocking tendency by binding the fibers with the matrix compared to AF/epoxy composites; this makes CAF-FCNT/epoxy composites more wear resistant.

Figure 4.20 shows that the wear surface contains much fiber when the load, frequency, and temperature are relatively low (30 N, 8 Hz, 30°C). Adhesion between the fibers and matrix material has caused degradation of the matrix material, resulting in fractures and wear debris, as seen in Figure 4.20. These fractures and wear debris occurred

due to repetitive back-and-forth motion over the same area, which created different signs of shear stress in each stroke. The main wear mechanism is adhesive wear, with some fiber abrasion taking place at low loads and frequencies.

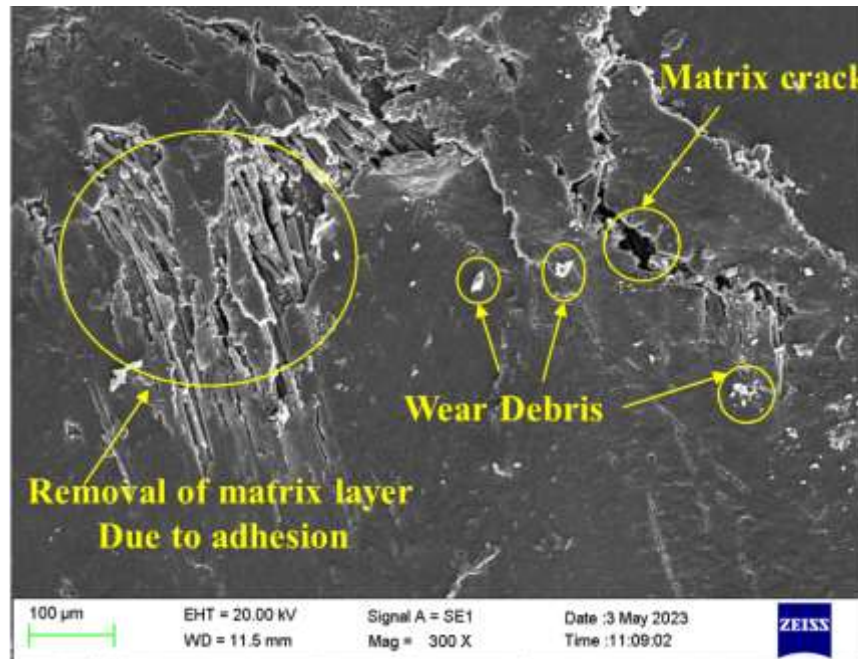


**Figure 4.20.** SEM of the worn surface of CAF-FCNT/epoxy polymer composites at (30N, 8Hz, 30°C)

#### 4.10 Summary

The findings of this chapter can be summarized as follows:

- Acid treatment (nitric and sulfuric) of aramid fibers and CNTs introduces functional groups, enhancing the bonding between them and promoting better interaction.
- CNTs coatings were applied on aramid fibers to improve interfacial characteristics, leading to enhanced mechanical integration of the polymer composite.
- CNT coating increases the surface roughness of aramid fibers, improving matrix interlocking and preventing micro-cracks and delamination, thus enhancing structural integrity.

- CNT coatings strengthen the bond with the epoxy matrix, resulting in a 22.9% increase in tensile modulus, a 23.3% boost in tensile strength, and a 32.41% reduction in specific wear rate.
- The friction coefficient increases with higher normal loads but decreases with temperature or sliding frequency.
- Significant improvements in hardness (27.27%) and thermal conductivity (36.56%) were achieved with CNT coatings.